Journal of the Korean Magnetic Resonance Society **2015**, *19*, 54-60
DOI 10.6564/JKMRS.2015.19.2.054

Structure-Activity Relationship of the N-terminal Helix Analog of Papiliocin, PapN

Dasom Jeon[1], Min-Cheol Jeong[1], Jin-Kyoung Kim[1], Ki-Woong Jeong[1], Yoon-Joo Ko[2], and Yangmee Kim[1]*

[1]Department of Bioscience and Biotechnology, Konkuk University, Seoul 143-701, South Korea
[2]National Center for Inter-University Research Facilities, Seoul National University, Seoul 151-742, South Korea

Received Aug 10, 2015; Revised Sep 15, 2015; Accepted Sep 25, 2015

Abstract Papiliocin, from the swallowtail butterfly, Papilio xuthus, shows high bacterial cell selectivity against Gram-negative bacteria. Recently, we designed a 22mer analog with N-terminal helix from Lys^3 to Ala^{22}, PapN. It shows outstanding antimicrobial activity against Gram-negative bacteria with low toxicity against mammalian cells. In this study, we determined the 3-D structure of PapN in 300 mM DPC micelle using NMR spectroscopy and investigated the interactions between PapN and DPC micelles. The results showed that PapN has an amphipathic α-helical structure from Lys^3 to Lys^{21}. STD-NMR and DOSY experiment showed that this helix is important in binding to the bacterial cell membrane. Furthermore, we tested antibacterial activities of PapN in the presence of salt for therapeutic application. PapN was calcium- and magnesium-resistant in a physiological condition, especially against Gram-negative bacteria, implying that it can be a potent candidate as peptide antibiotics.

Keywords Papillion, PapN, Antimicrobial peptide, Structure, NMR

Introduction

The increasing antibiotic resistant problem by commonly used antibiotics is a need for a novel antimicrobial agent which is not been exposed against microorganisms. Antimicrobial peptides (AMPs) are possible antibiotic candidates owing to they have broad spectrum antibacterial, antifungal and antiviral activities. To date more than 1500 AMPs have been discovered in all species, ranging from plants and insects to vertebrates.[1,2] They are being increasingly recognized as significant components of innate immunity in all living organisms.[3,4] Although the detailed mechanisms is not well understood, their mode of antibiotic action involves depolarization or permeabilization of the bacterial cell membrane, some AMPs can transverse intact membranes to interact with intracellular targets.[5-7]

Studies of innate immune systems of insects have shown the importance of AMPs for the defense of these organisms against bacteria.[7,8] In insects, over 200 AMPs have been identified. Papiliocin, with 37-residues (RWKIFKKIEKVGRNVRDGIIKAGPA VAVVGQAATVVK-NH2) has been isolated from the larvae of the swallowtail butterfly, Papilio xuthus, and it belongs to a cecropin family that have strong antibacterial activities against Gram-negative bacteria.[8] We studied the structure of papiliocin by NMR spectroscopy and the structure shows that

* Address correspondence to: **Yangmee Kim,** Department of Bioscience and Biotechnology, Konkuk University, Se oul 143-701, South Korea, Tel: 82-2-450-3421; E-mail: ymkim@konkuk.ac.kr

papiliocin has an α-helical structure from Lys^{3} to Lys^{21} and from Ala^{25} to Val^{35}, linked by a hinge region, in 300 mM dodecylphosphocholine (DPC) micelles.[9] In order to understand the structural requirements for papiliocin function and to design shorter and potent peptide antibiotics, we designed papiliocin analog, PapN (residues Arg^{1}-Ala^{22} from the N-terminal amphipathic helix).[10] PapN exhibited significant broad-spectrum antibacterial activities without cytotoxicity. Bactericidal kinetics of peptides against *E.coli* showed that papiliocin completely and rapidly killed *E.coli* in less than 10 minutes at 2 × MIC concentration, while PapN permeabilized bacterial membranes less effectively than papiliocin.[10] The results imply that the Trp^{2} and Phe^{5} in the amphipathic N-terminal helix are important in the rapid permeabilization of the gram-negative bacterial membrane.

In this study, to gain further insight into the structure-activity relationships, we determined the 3D- structures of PapN in 300 mM DPC micelles and investigated the interactions between DPC micelles and PapN. Finally, we investigated the therapeutic applications by testing the salt effect on PapN. We tested antibacterial activities of PapN in the presence of NaCl, $CaCl_2$ and $MgCl_2$ for therapeutic application. PapN was salt resistant and can be developed as a potent peptide antibiotics as useful therapeutic agents.

Experimental Methods

Peptide synthesis- Peptides were prepared by solid-phase synthesis using Fmoc (fluorenylmethoxycarbonyl) chemistry and purified by reversed-phase preparative high-performance liquid chromatography (HPLC) on a C18 column (20 × 250 mm; Shim-pack) as described previously.[9] The molecular mass of peptide was determined by matrix-assisted laser-desorption ionization-time-of-flight (MALDI-TOF) mass spectrometry (Shimadzu, Kyoto, Japan).

Antibacterial activity- Escherichia coli (KCTC 1682) and *Staphylococcus aureus* (KCTC 1621) were purchased from the Korean Collection for Type Cultures, Korea Research Institute of Bioscience & Biotechnology (Taejon, Korea). Minimum inhibitory concentrations (MICs) of peptide against these two bacteria were determined using a broth microdilution assay and compared with those of papiliocin as described in previous report.[7,9] Salt-resistance tests for peptides were also performed in the presence of NaCl, $CaCl_2$, or $MgCl_2$. MIC against two standard bacterial strains (*E. coli* KCTC 1682 and *S. aureus* KCTC 1621) were determined in the presence of 100–200 mM NaCl, 1 mM $CaCl_2$, and 1 mM $MgCl_2$.

NMR analyses and structure calculations- 1.0 mM PapN was dissolved in 9:1 (v/v) H_2O/D_2O 20 mM phosphate buffer, pH 5.9 containing 300 mM DPC micelles. We performed phase-sensitive two-dimensional experiments, including total correlation spectroscopy (TOCSY) and nuclear Overhauser effect spectroscopy (NOESY) using time-proportional phase incrementation.[11-14] 50 and 80 ms MLEV-17 spin-lock mixing pulses were used for TOCSY experiments and for NOESY experiments, mixing times of 250 ms and 350 ms were used. The $^{3}J_{HN\alpha}$ coupling constants were measured from the DQF-COSY spectra. Chemical shifts are expressed relative to the 4,4-dimethyl-4-silapentane-1-sulfonate signal at 0 ppm. Intramolecular hydrogen bondings in the peptides were investigated by calculating temperature coefficients from the TOCSY experiments at five different temperatures. All NMR spectra were recorded on a Bruker 600 MHz spectrometer (Bruker, Rheinstetten, Germany) at National Center for Inter-University Research Facilities at Seoul National University. NMR spectra were processed with NMRPipe[15] and visualized with Sparky.[16]

Using the standard protocol of Cyana 2.1 program in a LINUX environment, structure of PapN was calculated.[17] A total of 500 structures were calculated using the torsion angle dynamics protocol. The structures were sorted according to the final value of the target function, and the best 20 structures were

analyzed in terms of distance and angle violations.

Saturation transfer difference (STD) NMR experiments- STD-NMR experiments were recorded for 1.0 mM peptide in 300 mM DPC micelles on a Bruker 600 MHz spectrometer at a temperature of 298 K. The STD-NMR spectra were obtained with 512 scans and selective saturation of DPC resonances at -2.0 ppm (40 ppm for reference spectra). A cascade of 40 selective Gaussian-shaped pulses of 45-ms duration and a 100-ms delay between each pulse were used in all STD-NMR experiments with a total saturation time of 2 s. Subtraction of the two spectra (on resonance - off resonance) leads to the difference spectrum, which contains signals arising from the saturation transfer. Therefore, spectral differences primarily constituted resonances belonging to peptide protons bound to DPC micelles.

DOSY experiments- ^{1}H detected 2D DOSY data sets were recorded for 1.0 mM papiliocin in 300 mM DPC micelles on a Bruker 600 MHz spectrometer using the stimulated echo sequence with bipolar-gradient pulses and 32 T_1 blocks of 128 transients each as described previously.[18,19] The duration of the gradient pulse was 1.5 ms to obtain a 2 % residual signal with the maximum gradient strength. The 2D data sets were processed using BIOSPIN software.

Results

In our previous study, 3D-structure of papiliocin was determined in 300 mM DPC micelles and the result showed that papiliocin has an amphipathic α-helical structure from Lys^3 to Lys^{21} and hydrophobic α-helix from Ala^{25} to Val^{36}, a hinge region in between the helices.[9] To investigate the importance of N-terminal helical segments on its biological activities, we designed N-terminal analog, PapN from Arg^1 to Ala^{22} (Table 1). PapN has +1 net positive charge less than parent papiliocin and were more hydrophilic than the parent papiliocin. Trp^2 and Phe^5 in the amphipathic N-terminal helix are important for the antibacterial activities of papiliocin.[9,10]

Salt resistance tests- Since the reported concentrations of calcium and magnesium in human body fluids are on the order of 1 mM, it is important to determine MICs of PapN against bacteria in the presence of 1mM $CaCl_2$ and $MgCl_2$.[20] MIC of PapN against Gram-negative and Gram-positive bacteria in the presence of salt were measured and compared to those of papiliocin and melittin. As summarized in Table 2, PapN as well as papiliocin exhibited strong antibacterial activity against *E.coli* (Gram-negative bacteria). MICs were retained in the range of NaCl concentrations from 100 to 200 mM. However, against *S. aureus* (Gram-positive bacteria), MICs of PapN was significantly increased in the presence of NaCl while papiliocin did not show antibacterial activities against *S. aureus*. Even though the MICs of PapN against *E.coli* increased in the presence of 1 mM $CaCl_2$ and 1 mM $MgCl_2$, PapN as well as papiliocin showed good antimicrobial activity compared to melittin. Therefore, PapN can be described as calcium- and magnesium-resistant against Gram-negative bacteria at this concentration of $CaCl_2$ and $MgCl_2$, a physiological condition.

Resonance assignments and Structure of PapN- We performed sequence-specific resonance assignments of PapN using mainly DQF-COSY, TOCSY, and NOESY data, referencing by 4,4-dimethyl-4-silapentane-1-sulfonate, in 300 mM DPC micelles.[21,22] Fig. 2 shows the sequential assignments for PapN in the NH-NH region of

Table 1. Amino acid sequences and properties of the peptides.

Peptide	Sequence	MW	Net charge	Hydrophobicity
Papiliocin	RWKIFKKIEKVGRNVRDGIIKAGPAVAVVGQAATVVK-NH_2	4002.8	8	-1.48
PapN	RWKIFKKIEKVGRNVRDGIIKA-NH_2	2654.2	7	-2.10

NOESY spectra. The chemical shifts of PapN is very similar that of papiliocin. Sequential NOE connectivities and other NMR data are shown in Fig. 2. From Lys^3 to Lys^{21} for PapN, number of NOEs, such as $d\alpha_N(i,i+3)$ and $d\alpha_N(i,i+4)$ characterizing of an α-helix, were observed and these results suggest that

Table 1. MICs of papiliocin and PapN for bacteria determined in the presence of NaCl, $CaCl_2$, and $MgCl_2$

MIC (μM)				
Gram-negative				
Salt	Conc. (mM)	*E. coli*		
		Papiliocin	PapN	Melittin
none		0.50	1.0	4.0
NaCl	100	1.0	2.0	4.0
	150	2.0	4.0	8.0
	200	2.0	8.0	8.0
$CaCl_2$	1	1.0	4.0	32
$MgCl_2$	1	2.0	8.0	16
Gram -positive				
Salt	Conc. (mM)	*S. aureus*		
		Papiliocin	PapN	Melittin
None		32	8.0	4.0
NaCl	100	>32	32	4.0
	150	>32	>32	4.0
	200	>32	>32	4.0

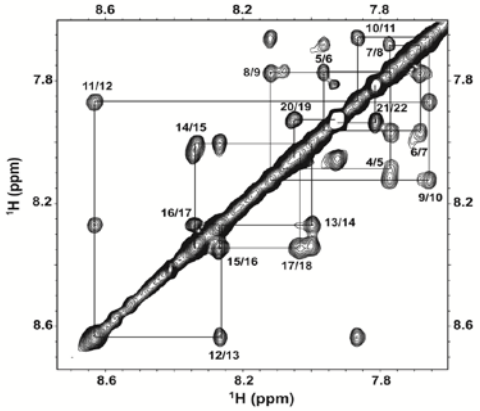

Figure 1. NOESY spectra of the NH-NH region of PapN in 300 mM DPC micelles at pH 5.9 and 303 K (mixing time, 250 ms).

the presence of an α-helix in this region. Furthermore, most of the residues of PapN have a negative ^{1}Hα Chemical Shift Index (CSI) determined using the method of Wishart et al.[23], indicating the presence of α -helix in these regions.

Figure 2. Summary of NOE connectivities and $C_\alpha H$ chemical shift indices for PapN in 300 mM DPC micelles. The thickness of the line for the NOEs reflects the intensity of the NOE connectivities.

Based on sequential (|i-j|=1), medium-range ($1<|i-j|\leq 5$), long-range (|i-j|<5) and intraresidual distance restraints, the tertiary structures of PapN was calculated. Hydrogen bonding restraints as well as torsion angle restraints were included, too. When the 20 lowest-energy structures of PapN were superimposed over the backbone atoms for residues Lys^3 to Lys^{21} (Fig. 3A), the root mean squared deviations from the mean structures were 0.04 ± 0.03Å for the backbone atoms (N, Cα, C', O) and 0.80 ± 0.09Å for all heavy atoms, respectively (Table 3). Fig. 3B shows the ribbon diagram of PapN and papiliocin, and the amphipathic α-helical structure of N-terminal helix is the very similar in both peptides. Fig. 3C shows a head-on view of the amphipathic α-helix of PapN from residue Lys^3 to Lys^{21}. According to a Procheck analysis, PapN exhibited an amphipathic helices from Lys^3 to Lys^{21}.

NMR studies of peptide bound to DPC micelle- To understand the mode of peptide interaction with DPC micelle, we performed STD-NMR experiments. Fig. 4 showed the one-dimensional spectra of free peptide and the STD spectra of peptide bound to DPC micelle. Spectral differences primarily constituted resonances belonging to peptide protons bound to DPC

micelle. The STD spectrums of PapN showed aromatic ring protons of Trp and Phe as well as the amide protons from most residues in PapN, and a number of aliphatic side-chain proton resonances are having close associate with DPC micelle.

Table 2. Structural statistics and mean pairwise root mean squared deviations for the 20 lowest-energy structures of PapN in 300 mM DPC solution at 303 K.

Distance restraints		
Intraresidue (i-j=0)		127
Sequential (|i-j|=1)		130
Medium-range (2≤|i-j|≤4)		107
Total		357
H-bond		26
Angular restraints (Φ)		18
Mean Cyana target function (Å^2)		0.3±0.0007
Deviation from mean structure		
	Residues 3–21	Residues 1–22
Backbone atoms	0.24 ± 0.13	0.04 ± 0.03
Heavy atoms	1.05 ± 0.13	0.80 ± 0.09
Ramachandran plot for the mean structure		
Residues in the most favorable and additionally allowed region (%)		100.00

NMR studies of peptide bound to phospholipid membrane- Since papiliocin include N-terminal helix, PapN as well as C-terminal helix, we investigate the interactions between papiliocin and phospholipid membrane using DOSY experiments. The 2D data sets were processed with the two-exponential decays using the BIOSPIN software and consisted of an exponential-multiplication apodization function in the F_2 dimension (lb = 1 Hz), prior to Fourier transformation. The NH region of the 1D and DOSY spectra of the papiliocin in a 9:1 (v/v) H_2O/D_2O and papiliocin in DPC micelles are shown in Fig. 5. As illustrated in the spectra of papiliocin, addition of DPC resulted in better dispersions in chemical shift of spectrum compared to that in H_2O/D_2O. These changes imply that papiliocin has unfolded structures in aqueous solution while they form α-helical structure in micellar environments which mimic the amphipathic environment of a phospholipid bilayer. The T_1 diffusion dimension was processed by fitting the intensity of the resultant F_2 peaks using the equation reported by Morris et al.[19] In aqueous solution the diffusion coefficient of the peptide was in the range from 3.1×10^{-10} to 6.9×10^{-10} m^2s^{-1} while in DPC micelle it was in the range from 6.6×10^{-11} m^2s^{-1} to 7.9×10^{-11} m^2s^{-1}. Therefore, the diffusion coefficients of most residues in peptide were decreased much when bound to DPC micelles. This result suggested that both N-terminal helix and C-terminal helix in papiliocin interact with DPC micelles and diffuse slowly in bound form.

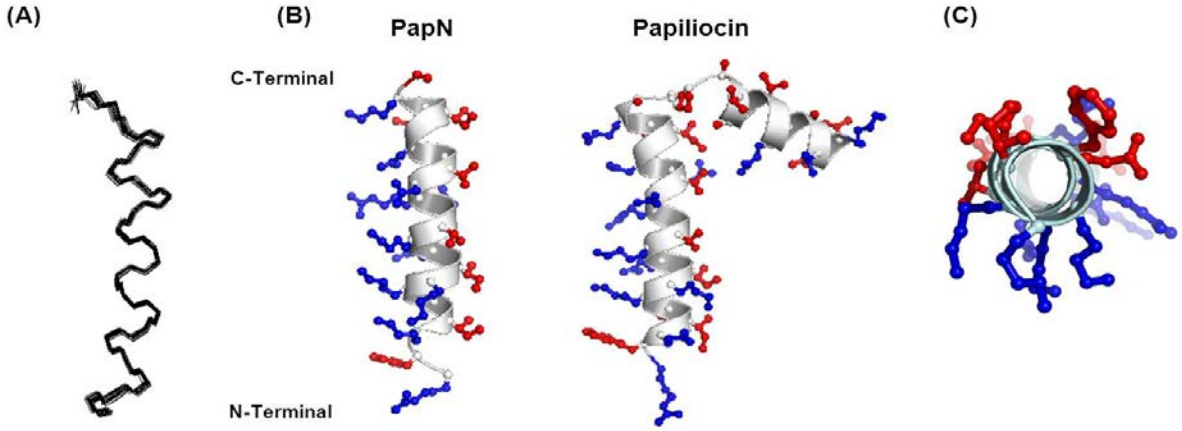

Figure 3. (A) The superpositions of the 20 lowest-energy structures calculated from the NMR data for PapN in 300 mM DPC micelles. The backbone atoms of residues Lys^3 to Lys^{21} are superimposed. (B) Hydrophobic surface model of PapN and papiliocin. The hydrophobic and hydrophilic side-chains are indicated in red and blue, respectively. (C) Head-on view of the amphipathic N-terminal helix from Lys^3 to Lys^{21} of PapN.

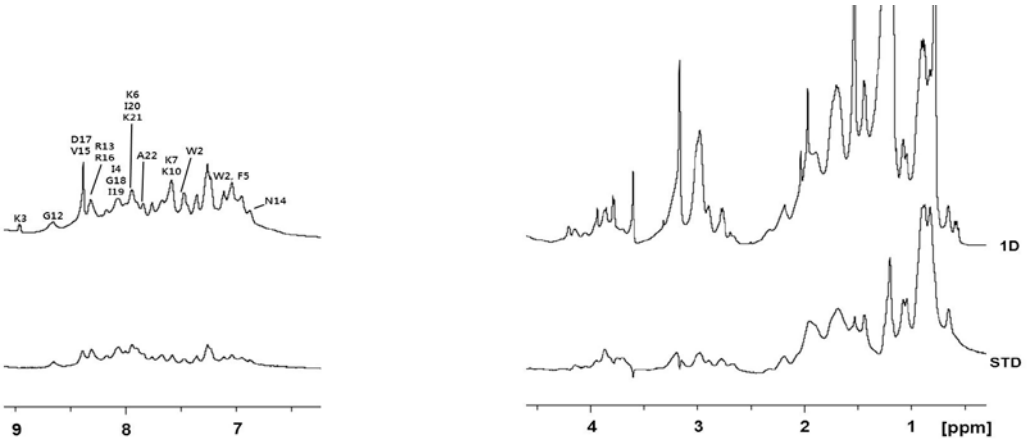

Figure 4. STD-NMR results showing the interaction between 1.0 mM PapN peptide and 300mM DPC micelle in amide protons and aromatic protons as well as the aliphatic protons.

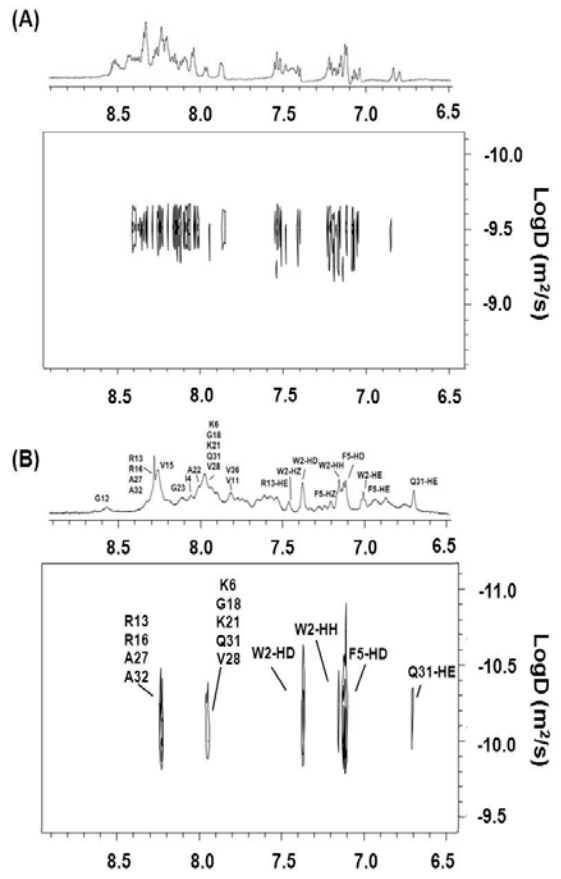

Figure 5. The NH region of the 1H 1D spectra and DOSY spectra for (A) papiliocin in a 9:1 (v/v) H_2O/D_2O and (B) papiliocin in 200 mM DPC micelles at 298 K.

Discussion

In this study, we examined the antimicrobial activity of PapN in the presence of salt. It has been reported that the NaCl concentration in the environment of the epithelial cells of cystic fibrosis patients is 120 mM, the interactions between AMPs and the LPS components of the outer membrane of Gram-negative bacteria are inhibited by high concentrations of salt.[20] From salt-resistance experiments, it was shown that even at high salt concentrations, PapN retained its antibacterial activity against Gram-negative bacteria. Because high ionic concentrations generally found in body fluids of patients with inflammatory disease, PapN may be a potent antibiotic candidate for use in patients with inflammatory disease. However, PapN does not show good antibacterial activity against Gram-positive bacteria and it is highly selective against Gram-negative bacteria similar to papiliocin.

Using NMR spectroscopy, the structure of PapN in 300 mM DPC micelles was determined, having a stable linear amphipathic α-helical structure from Lys^3 to Lys^{21}. This amphipathic character of PapN should the critical factor to interact with lipid membrane. In this study, STD-NMR experiments as well as DOSY experiment demonstrated that most residues as well as Trp^2 and Phe^5 in PapN are in close

contact with DPC micelle and the amphipathic helix of PapN is important in interactions with the bacterial cell membrane.

In conclusion, N-terminal helix region in papiliocin is essential for its antimicrobial activity and interaction with bacterial cell membrane. PapN was salt resistant and can be described as calcium- and magnesium-resistant against Gram-negative bacteria in a physiological environment, implying that it can be developed as a potent candidate for peptide antibiotics against Gram-negative bacteria.

Acknowledgements

This work was supported by grants from the Basic Science Research Program (2013R1A1A2058021) through the National Research Foundation of Korea, funded by the Ministry of Education, Science, and Technology.

References

1. E. Guaní-Guerra, T. Santos-Mendoza , S. O. Lugo-Reyes, and L. M. Terán , *Clin Immunol.* **135**, 1 (2010)
2. P. Bulet, R. Stöcklin, and L. Menin, *Immunol Rev.* **198**, 169 (2004)
3. R. E. Hancock, and R. Lehrer, *Trends Biotechnol.* **16**, 82 (1998)
4. S. E. Blondelle, K. Lohner, and M. Aguilar, *Biochem Biophys Acta.* **1462**, 89 (1999)
5. R. E. Hancock, and H. G. Sahl, *Nat Biotechnol*. **24**, 1551 (2006)
6. K. A. Brogden, *Nat Rev Microbial.* **3**, 238 (2005)
7. E. Lee, J.-K. Kim, S. Shin, K.-W. Jeong, A. Shin, J. Lee, D. G. Lee, J.-S. Hwang, and Y. Kim, *Biochem Biophys Acta.* **1828**, 271 (2013)
8. S. R. Kim, M. Y. Hong, S. W. Park, K. H. Choi, E. Y. Yun, T. W. Goo, S. W. Kang, H. J. Suh, I. Kim, and J. S. Hwang *Mol. Cells* **29**, 419 (2010)
9. J.-K. Kim, E. Lee, S. Shin, K.-W. Jeong, J.-Y. Lee, S.-Y. Bae, S.-H. Kim, J. Lee, S. R. Kim, D. G. Lee, J.-S, Hwang, and Y. Kim, *J. Biol. Chem.* **286**, 41296 (2011)
10. E. Lee, J.-K. Kim, D. Jeon, K.-W. Jeong, A. Shin, and Y. Kim, *Scientific reports*. **5**, 12048 (2015)
11. A. Derome, and M. Williamson, *J.Magn. Reson*. **88**, 177 (1990)
12. A. Bax and D. G. Davis, *J. Magn. Reson*. **65**, 355 (1985)
13. A. Bax and D. G. Davis, *J. Magn. Reson*. **64**, 207(1985)
14. D. Marion and K. *Wüthrich, Biochem Biophys Res Commun*. **113**, 967 (1983)
15. F. Delaglio, S. Grzesiak, G. Vuister, G. Zhu, J. Pfeifer, and A. Bax, *J. Biomol. NMR*. **6**, 277 (1995)
16. T. D. Goddard and D. G. Kneller, *Sparky 3*, University of California, SanFransisco, CA.
17. P. Güntert, *Methods Mol Bio*. **278**, 353 (2004)
18. J.-K. Kim, E. Lee, K.-W. Jeong, and Y. Kim *J. Kor. Mag. Reson. Soc*. **15,** 1 (2011)
19. K. F. Morris and C. S. Johnson, *J. Am. Chem.***114**, 3139 (1992)
20. A. M. Cole, R. O. Darouiche, D. Legarda, N. Connell, and G. Diamond *Antimicrob. Agents. Chemother*. **44**, 2039 (2000)
21. W. Kim, J. Rhee, J. Yi, B. Lee, and W. Son, *J. Kor. Mag. Reson. Soc*. **18,** 36 (2014)
22. K. Lee and J. Suh, *J. Kor. Mag. Reson. Soc.* **19,** 42 (2015)
23. D. S. Wishart, B. D. Sykes, and F. M. Richards, *Biochemistry*. **31**, 1647-1651 (1992)